Combining Theory and Experiment to Study the Photooxidation of Polyethylene and Polypropylene

Monica Bertoldo,[†,‡] Simona Bronco,[†,‡] Chiara Cappelli,*[,†,‡] Tania Gragnoli,[‡] and Leonardo Andreotti[§]

INFM, Istituto Nazionale per la Fisica della Materia, Unità di Ricerca di Pisa, Via Risorgimento 35, I-56126 Pisa, Italy, Dipartimento di Chimica e Chimica Industriale, Università di Pisa, Via Risorgimento 35, I-56126 Pisa, Italy, and Gruppo X di X Gruppo, c/o Parco Scientifico Tecnologico Vega, Via della Libertà 5/12, I-30175 Marghera (VE), Italy

Received: May 23, 2003; In Final Form: August 28, 2003

A methodology, which combines experimental evidence and theoretical calculations, able to give a molecular interpretation and a quantification of the photooxidation of polyolefins is here derived. The methodology involves the analysis of experimentally recorded infrared spectra in combination with density functional theory calculations. Environmental effects are taken into account by exploiting the polarizable continuum model. A test against polyethylene and polypropylene samples UV-irradiated under the conditions used for the photocoating is reported. The results obtained with the combined theoretical/experimental methodology are in good agreement with previous findings obtained by exploiting more complex purely experimental approaches.

1. Introduction

In this paper a novel methodology, which combines experimental evidence and theoretical calculations, to obtain a molecular interpretation and a semiquantitative analysis on photooxidation of polyolefins is suggested.

The oxidation of polyolefins has been the subject of studies for many years (see for example ref 1). From the experimental point of view, the most used tool is infrared (IR) spectroscopy,[2] but also mass spectroscopy[3] and ^{13}C NMR[4] have been employed. In the IR analysis of photooxidized polyolefins three regions of the middle infrared spectrum are considered: the ranges of the O−H stretching modes, the range of the C═O stretching modes, and the ranges of the rocking of the double bonds. The range of the C═O stretches is particularly interesting, since oxidation leads to the appearance of a broad band with several maxima between 1700 and 1800 cm^{-1}.

The mechanism commonly invoked in the oxidation process of polyolefins is the attack of free radicals on the polymer chain. The alkyl radicals generated in this way react with oxygen, giving rise to hydroperoxides, alcohols, and carbonyl compounds such as carboxylic acids, ketones, and esters, whose relative percentage depends on oxidation conditions.[1] Although the nature of oxidation products is quite well understood, the quantification of each product is difficult to establish unambiguously. This is due to the fact that in the IR spectrum of the oxidized polymer the bands of the various oxidation products overlap into broad bands.

The quantification of the various oxidation products of polyethylene (PE) and polypropylene (PP) (as a result of gamma, photo, and thermal oxidation) has been done by Lacoste et al.[5,6] by combining IR spectroscopy and chemical derivatization. These studies revealed that PE oxidation yields predominantly ketones with lesser amounts of secondary hydroperoxides and carboxylic acids, whereas PP gives predominantly tertiary hydroperoxides and lesser secondary peroxides and ketones. In addition, in the case of PP, carboxylic acids are of minor importance, except in the case of a high degree of oxidation. More recently Philippart et al.[7] used Fourier transform infrared spectroscopy (FTIR) coupled with chemical derivatization to quantify degradation products of PP resulting from UV irradiation. The findings of this study were that, depending on the exposure parameters (light intensity and exposure time), changes in the kinetics of the photooxidation arise, as well as modifications in the relative concentrations of the various oxidation products. In particular, the concentration of carbonylated compounds, such as carboxylic acids and esters, is largely dependent on exposure parameters.

In this study a different combination of techniques is used: in particular experimental IR spectra are analyzed in combination with density functional theory (DFT) calculations.

The methodology reported here has two aims. The first is to rationalize IR spectra of oxidized polymers in terms of the nature of the oxidation products. The second (more ambitious) is to quantify the various oxidation products so as to rationalize their formation in terms of chemical intuition. As an example of application, the methodology will here be tested against polyethylene and polypropylene samples UV-irradiated under the conditions used for the photocoating (the films were exposed to high-intensity UV radiation for limited periods of time, from 40 min up to 6 h), but may be easily applied to any kind of polymers and oxidation conditions (gamma or UV irradiation, thermal oxidation).

2. Methodology

As already mentioned in the Introduction, the photooxidation of polymers is usually studied by resorting to IR spectroscopy. This is mainly due to the simplicity and widespread availability of IR instrumentation coupled with the fact that oxidation products of polyolefins give rise to strong bands in the IR range.

* Corresponding author. E-mail: chiara@dcci.unipi.it.
† INFM, Istituto Nazionale per la Fisica della Materia.
‡ Dipartimento di Chimica e Chimica Industriale, Università di Pisa.
§ Gruppo X di X Gruppo.

10.1021/jp035427h CCC: $25.00
Published on Web 10/07/2003

The molecular interpretation and quantification of the oxidation process requires IR spectroscopy to be coupled with other techniques. In fact, first the assignment of the various bands to specific oxidation products is not trivial. In addition, once the assignment has been done, the quantitative determination of each oxidation product can be done by resorting to the Lambert−Beer law, which connects the absorbance of the band A to the concentration of the species, c, to an experimental parameter, namely, the optical path, l, and to the molar extinction coefficient of the species, ϵ:

$$A = \epsilon l c \tag{1}$$

Thus, to quantify oxidation products, both their nature and their molar extinction coefficients should be known.

A useful procedure to both assign the bands of a spectrum and evaluate molar extinction coefficients is to rely on theoretical calculations, and this is the technique we will exploit here.

2.1. Choice of the Theoretical Level. The choice of the level of theory to exploit in the calculations crucially determines the quality of the results one can obtain. Such a choice should be done by carefully considering the features of the physical phenomenon under investigation. In our case, we would like to reproduce IR spectra (both frequencies and intensities), and thus one has to choose a theoretical level able to model molecular vibrations. It is generally accepted that, still relying on a purely harmonic model, the theoretical description of molecular vibrations requires the use of quantum mechanical calculations of quite high level.

Much interest has been given to the problem of theoretically predicting vibrational spectra of organic molecules. In particular, the performances of various quantum mechanical levels have been tested against experimental values for IR frequencies by Scott and Radom,[8] who made a comprehensive study on 1066 vibrational frequencies of organic compounds of different nature. What is generally noticed is that ab initio harmonic vibrational frequencies are usually larger than experimental values, due to the neglect of anharmonicity in the theoretical treatment and to errors arising from the choice of the theoretical level and from the use of finite basis sets. Such an overestimation is quite uniform, and for this reason the use of generic scale factors to compare calculated and experimental data is commonly done. Particularly used in this framework is DFT with hybrid functionals, which for a given basis set has been proven to provide results of similar quality (or even superior) to highly correlated quantum mechanical levels (such as MP2, second-order Möller−Plesset perturbation theory) at a much lesser computational cost.

Regarding the prediction of IR intensities, the performance of DFT has been assessed by Halls and Schlegel,[9] by comparing computed intensities with results from conventional correlated ab initio methods. Similarly to frequencies, also for IR intensities DFT gives results comparable to MP2 at a much lesser computational cost.

2.2. Choice of the Model Systems. The need to use high-level computational models to treat molecular vibrations in principle contrasts with the possibility of studying large (macro)-molecules, like PE and PP. In general quantum mechanical calculations are not accessible for polyolefins, unless periodic boundary conditions are used.[10] In our case, however, such a model could not be exploited: in fact, the photooxidation of polyolefins performed under our conditions would reasonably lead to monooxidized compounds (such as monoketones, esters, acids, etc). The use of periodic boundary conditions would have permitted the modeling of polyoxidized compounds (polyketones, esters, acids, etc.), leading to incorrect results. For this reason we have resorted to "classical" quantum mechanical calculations, by redefining the model systems according to the physics and chemistry of the process and to the available computational resources.

Similarly to the choice of the theoretical level of description, also the choice of the model systems crucially affects the quality of the results one can obtain. In our case we are interested in the C═O stretching mode of carbonyl and carboxyl compounds and in the rocking vibration of carbon double bonds. Because such vibrations are quite "localized" in the molecule, i.e., they involve motions of the part of the molecule near the functional group responsible for them, it is reasonable, in our opinion, to model the oxidized systems in terms of a small molecule bearing the appropriate functional group (carbonyl group of ketonic, esteric, acid, etc., nature) and having the lateral chain(s) modeled on the structure of PE or PP monomers, but limited as much as possible in length.

2.3. Effect of the "Environment". To improve the basic model we have presented, we need a method to take into account that we are not dealing with small isolated molecules but with macromolecules resulting from the oxidation of PE or PP in a polymeric matrix. We have thus to consider two refinements in our model: (1) the real systems we are studying are much larger than the model systems, so a method to take into account the effect of the "remaining" part of the molecule (not present in the basic model) should be used; (2) the oxidized macromolecules are surrounded by other macromolecules, and the effect of this kind of "environment" should be considered.

In this paper both the effects just mentioned will be accounted for by refining the model so as to consider the small model molecules discussed in the previous section surrounded by a medium with the characteristics of PE or PP. To model the environment, among the various models present in the literature we will exploit here the polarizable continuum model (PCM),[11] which considers the medium as a continuum, infinite, homogeneous, and generally isotropic dielectric. The molecule, which is a sort of "solute", is assumed to be inside a molecular-shaped cavity, and the electrostatic solute−solvent interactions are calculated in a self-consistent way; that is, the molecule and the "environment" are mutually equilibrated. Notice that such a model has been developed for the calculation of interactions in liquid phase: in this case it has been proven to give reliable results for both energetic quantities[12] and molecular properties (absorption and emission spectra, scattering processes, magnetic properties, nonlinear optical properties, etc.),[13] but it has never been exploited so far to model molecule−environment interactions in solid or semisolid phase. However, some point should be stressed to validate our procedure. In particular, in this paper we are interested in modeling and quantifying oxidation products arising from the photooxidation of polyolefins. It is reasonable to consider that the oxidation occurs in the noncrystalline part of the sample;[14] thus the oxidation products will probably be immersed in a semisolid amorphous phase. In this case, the modeling of such a phase as a dielectric medium, having the dielectric properties of PE or PP, should be reasonable, at least as a first approximation. Obviously all the peculiar features of the system arising from the crystalline phase will be discarded by our model.

3. Experimental and Computational Details

PP and PE films kindly supplied by bpEuropack s.p.a., Lugo di Vicenza, Italy, with a thickness of 20 μm, were irradiated from 5 min to 6 h with a mercury vapor UV lamp at medium

pressure and a power of 100 W/cm. The irradiance intensity of the lamp at a distance of 30 cm was 3500 W/cm^2 at a wavelength of 365 nm. Notice that the intensity of the lamp used here is much higher than intensities usually exploited in Xenon tests.

The samples were prepared by superimposing three times a portion of the film obtained by cutting it around the irradiation center. After that the samples were put in a heated hot plane press at 80 °C to obtain a multilayer. FTIR spectra were measured with a Perkin-Elmer Spectrum One spectrometer interfaced with a PC. For each spectrum 24 scan were done. The spectra in the range of the C═O stretches were corrected by using as reference the spectra of PE and PP measured after 5 min of irradiation; in fact after this time bands connected to antioxidant species present in the commercial polyolefins disappear. The spectra were normalized with respect to the absorption band at 1304 cm^{-1} for PE and 1256 cm^{-1} for PP.

The absorbance values reported in the following were obtained by measuring the area of the various bands.

Quantum mechanical calculations were performed by using DFT with the B3LYP hybrid functional and the 6-31+G* basis set. Extensive analysis of the effect of the choice of the functional and of the basis set for gas phase IR calculations are available in the literature.[8,9]

The calculations taking into account "environmental" effects were done by using PCM.[11] The geometries of all the species were optimized both in the gas and in the condensed phase. The calculations of infrared frequencies and intensities in solution were performed by considering the coupling between the radiation electric field and the solvent in the complete nonequilibrium framework, as reported in refs 15 and 16. The molecular cavity used was of molecular shape and built by interlocking spheres. The radii of the spheres were 2.4 Å for methyl and methylene groups, 2.04 Å for methyne groups, 1.8 Å for oxygen, and 2.04 Å for the carbon atom belonging to the carbonyl group.

A development version of the Gaussian program[17] was used for all the calculations.

4. Results and Discussion

4.1. Experimental Findings. The analysis of FTIR spectra of PP and PE films before and after irradiation shows, as expected, the appearance of absorption bands in the region of C═O stretching modes (1650−1850 cm^{-1}) for PE and PP and changes in the absorption pattern in the region of the carbon double bond rocking modes (850−1050 cm^{-1}) for PE. The behavior of the spectrum in such regions as a function of irradiation time is reported in Figures 1, 2, and 3, respectively.

By analyzing Figures 1 and 2, it is clear that, with increasing the irradiation time a strong increment of the absorbance in the region of the C═O stretches is noticed. Also the shape of the absorption band changes as the oxidation time increases. It should be noticed that the shape of the C═O band is complex, this meaning that this band is due to carbonyl-containing species of various nature (ketones, aldehydes, esters, acids, etc.). In particular, in the case of PP (Figure 2) a rapid increase of a band around 1721 cm^{-1} is noticed, as well as the increase of the absorbance around 1780 cm^{-1}. Rapid changes in the C═O band (both shape and intensity) are noticed also in the case of PE (Figure 1). However, for PE no relevant changes are noticed beyond 1760 cm^{-1}. In addition, the intensity of the whole band is smaller in the case of PE than in the case of PP, showing, at least at first glance, a lesser oxidizability of PE with respect of PP. This is not surprising, being well documented in the literature.[1] More information on PE can be obtained by considering the carbon double bond rocking region (see Figure 3). In this case, we notice an increase in the intensity of the bands at 993 and 909 cm^{-1} and a decrease of the absorbance at 889 and 964 cm^{-1}. This behavior means that double-bond-

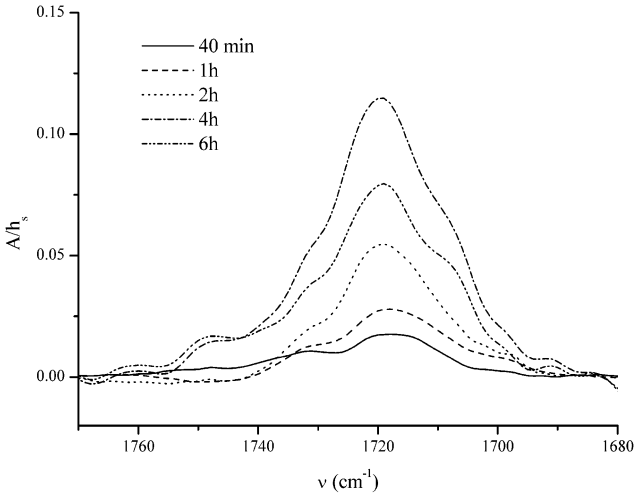

Figure 1. Experimental spectrum of PE in the region of the C═O stretches recorded after different times of exposure to UV radiation.

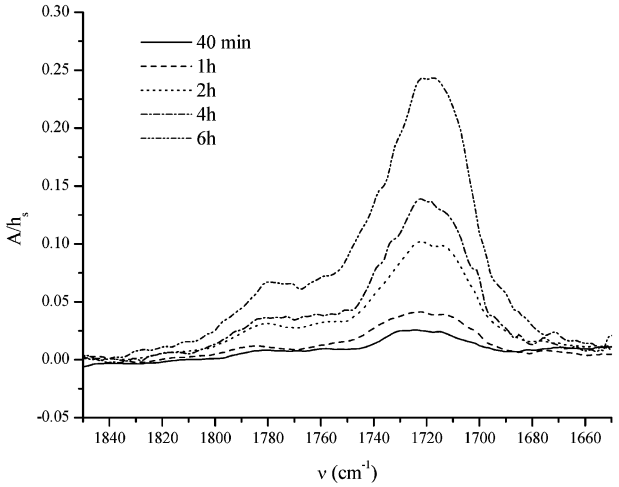

Figure 2. Experimental spectrum of PP in the region of the C═O stretches recorded after different times of exposure to UV radiation.

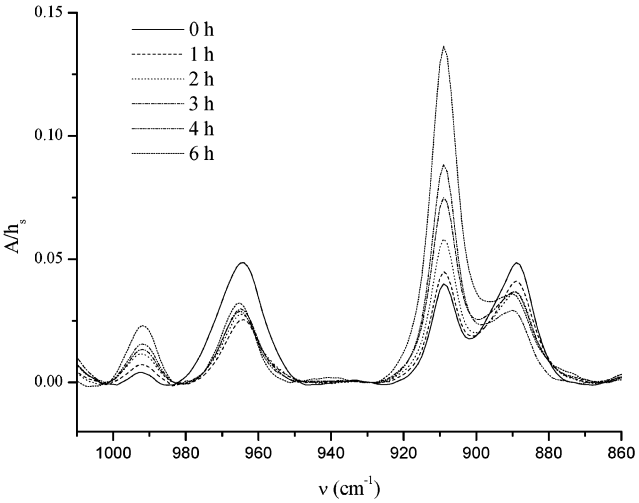

Figure 3. Experimental spectrum of PE in the region of the C═C rocking modes recorded after different times of exposure to UV radiation.

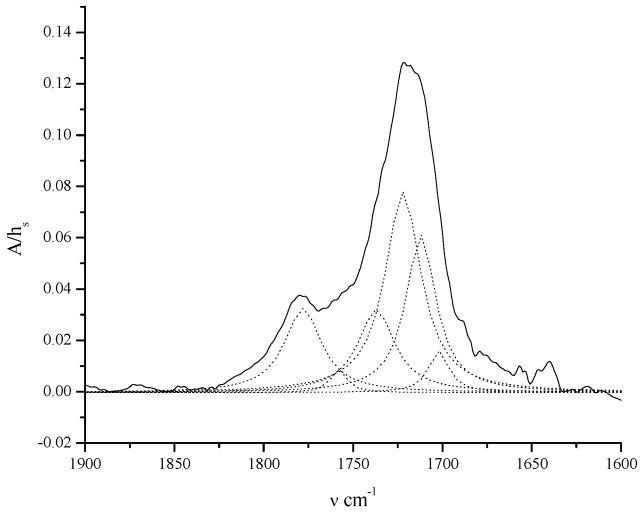

Figure 4. Results of the deconvolution procedure applied to the C═O stretches region of the IR spectrum of PP after 4 h of exposure to UV light.

TABLE 1: Summary of the Assignment Present in the Literature of the Various Bands Arising from Deconvolution of the IR Spectrum of Photooxidized PE

exptl freq (cm^{-1})	ref 5
1718	internal ketone
1724	terminal ketone
1744	ester
1784	γ-lactone
909, 995	vinyl ($-CH{=}CH_2$)
888	vinylidene ($>CH{=}CH_2$)
965	*trans* vinylene ($-CH{=}CH-$)

containing species are originally present in the film but that the concentration of these species varies as the oxidation proceeds.

Starting from this evidence, what we want to do in the following is to try to rationalize and explain the behavior just discussed.

A deconvolution procedure applied to the broad band that appears in the C═O stretching region of FTIR spectra yielded two Lorentzian-shaped bands centered at 1713 and 1721 cm^{-1} in the case of PE and six Lorentzian-shaped bands centered at 1702, 1712, 1722, 1737, 1758, and 1778 cm^{-1}, whose absorbance varies by increasing the irradiation procedure. As an example, in Figure 4 we show the result of the deconvolution procedure for PP irradiated for 3 h.

This procedure leads to results very similar to those found by Philippart et al.,[7] who reported the deconvolution of the C═O stretching band of oxidized PP (under different conditions than those used in the present study) in terms of seven bands centered at 1640, 1700, 1713, 1720, 1735, 1755, and 1780 cm^{-1}.

The next step in our analysis is the assignment of the various bands. To this end, we will resort to quantum chemical calculations on model systems, as already mentioned previously.

4.2. Assignment of the Bands. For the choice of the model systems to consider we have followed the assignment of the bands arising from the deconvolution reported in refs 5−7, which are summarized in Table 1 for PE and in Table 2 for PP; in addition we have also done calculations on other compounds, not mentioned in the cited references, but which can help us in making the assignment (see below). As we are interested mainly in describing the C═O stretch and the rocking vibration of carbon double bonds, which are quite "localized" motions in the molecule, we used as model systems small molecules bearing

TABLE 2: Summary of the Assignment Present in the Literature of the Various Bands Arising from Deconvolution of the IR Spectrum of Photooxidized PP

exptl freq (cm^{-1})	ref 6	ref 7
1702		unsaturated ketone
1712	carboxylic acid (dimeric form)	carboxylic acid (dimeric form)
1722	ketone (internal and terminal)	ketone (internal and terminal)
1737	ester or peroxy acid	ester
1758	ester or peroxy acid	carboxylic acid (free form)
1778	peroxy ester or γ-lactone	γ-lactone

TABLE 3: B3LYP/6-31+G(d) Calculated Harmonic Carbonyl Stretching Frequencies (cm^{-1}) and Intensities (km/mol) for a Series of PE-Type Terminal Ketones

system	frequency	intensity
CH_3COCH_3	1794	199.00
$CH_3COCH_2CH_3$	1791	166.86
$CH_3CO(CH_2)_2CH_3$	1791	166.86
$CH_3CO(CH_2)_3CH_3$	1789	164.50
$CH_3CO(CH_2)_4CH_3$	1789	165.06
$CH_3CO(CH_2)_5CH_3$	1789	163.27
$CH_3CO(CH_2)_6CH_3$	1789	163.06

the appropriate functional group (carbonyl group of ketonic, esteric, acid, etc., nature, carbon double bond) with a small lateral chain(s) modeled on the structure of PE or PP monomeric units. The length of the lateral chain has been chosen in the following way. Taking as an example of the compounds under examination a linear terminal ketone, we have performed frequency calculations starting from acetone and lengthening the lateral chain by one $-CH_2-$ group at a time. The results we have obtained from such calculations are reported in Table 3, which shows that as the number of C atoms in the lateral chain increases, the difference in frequency and intensity values decreases. When the lateral chain is made of at least four carbon atoms, such values can be considered almost constant. Starting from these findings and considering the computational resources at our disposal, we have chosen to use the model compounds shown in Figures 5 and 6 for PE and PP, respectively.

In Tables 4 and 5 we report calculated frequencies and intensities of the C═O stretching vibration and of the carbon double bond rocking in the case of PE for all the molecules shown in Figures 5 and 6. Starting from these data, it is possible to attempt assigning the various bands resulting from the deconvolution of the spectrum to a specific functional group. However, some features of the calculated data make the assignment not so trivial. As already mentioned in section II, calculated harmonic vibrational frequencies are usually larger than experimental values. This behavior is confirmed by the data reported in Tables 4 and 5. However, it is generally noticed that the overestimation of the experimental value is quite uniform, so that it is reasonable to assume that the "hierarchy" of the frequencies of the various compounds is reliably predicted.

Calculated data for PP (where only the C═O stretching band is of interest, Table 5) show that the frequency increases in the following order: internal unsaturated ketones < terminal unsaturated ketones < internal ketones < terminal ketones < esters < aldehydes < peroxy acids < peroxy esters < carboxylic acids < lactones. As a starting point let us consider the band at 1722 cm^{-1}, which has been assigned in both refs 6 and 7 to ketones. This assignment would lead to a scaling factor from calculated to experimental data ranging from 0.9631 to 0.9647 depending on the type of ketones (terminal or internal) chosen as reference.

TABLE 4: B3LYP/6-31+G(d) Calculated Harmonic Carbonyl Stretching Frequencies (cm^{-1}) and Intensities (km/mol) for Simple PE-Type Model Molecules

		isolated molecule		with medium effects	
		freq	int	freq	int
1	ketone: internal	1785	138.57	1769	210.21
2	ketone: terminal	1789	165.06	1771	231.67
3	uns. ketone: internal	1685−1767	222.07−126.13	1672−1749	261.98−156.24
4	uns. ketone: terminal	1679−1771	64.17−108.31	1674−1756	88.09−150.14
5	aldehyde	1806	226.75	1786	274.05
6	carboxylic acid	1855	255.74	1826	338.06
7	ester	1792	244.27	1761	326.06
8	lactone	1846	357.40	1816	441.82
9	trans vinylene −CH═CH−	991−1010	22.94−17.89	990−1009	32.08−26.56
10	vinyl −CH═CH_2	936−940−1027	37.16−12.69−11.94	931−1025−1030	62.50−15.55−3.73
11	vinylidene >C═CH_2	921	36.26	914	46.72

TABLE 5: B3LYP/6-31+G(d) Calculated Harmonic Carbonyl Stretching Frequencies (cm^{-1}) and Intensities (km/mol) for Simple PP-Type Model Molecules

		isolated molecule		with medium effects	
		freq	int	freq	int
1	ketone: internal	1778	136.72	1762	214.40
2	ketone: terminal	1788	149.43	1771	221.43
3	uns. ketone: internal	1662−1742	283.19−141.24	1655−1738	327.29−179.40
4	uns. ketone: terminal	1678−1769	67.21−93.47	1672−1755	89.14−141.76
5	aldehyde	1806	187.21	1786	242.44
6a	carboxylic acid, free form	1847	242.95	1819	333.34
6	carboxylic acid, *h*-bonded form[a]	1771	271.71	1767	373.82
7	ester	1787	242.43	1760	323.78
8	peroxy acid	1828	224.18	1805	304.67
9	peroxy ester	1835	203.20	1818	318.44
10	lactone	1844	367.68	1815	452.57

[a] "Expected values", see text for explanation.

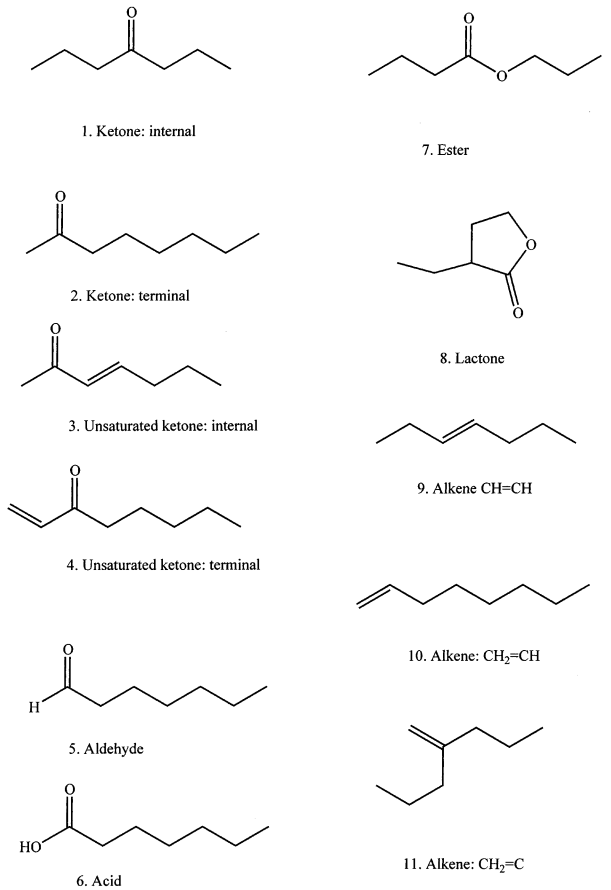

Figure 5. Structures of the PE-type model systems.

Such values are very similar to those reported by Scott and Radom in ref 8 for frequency at the B3LYP/6-31G* level.

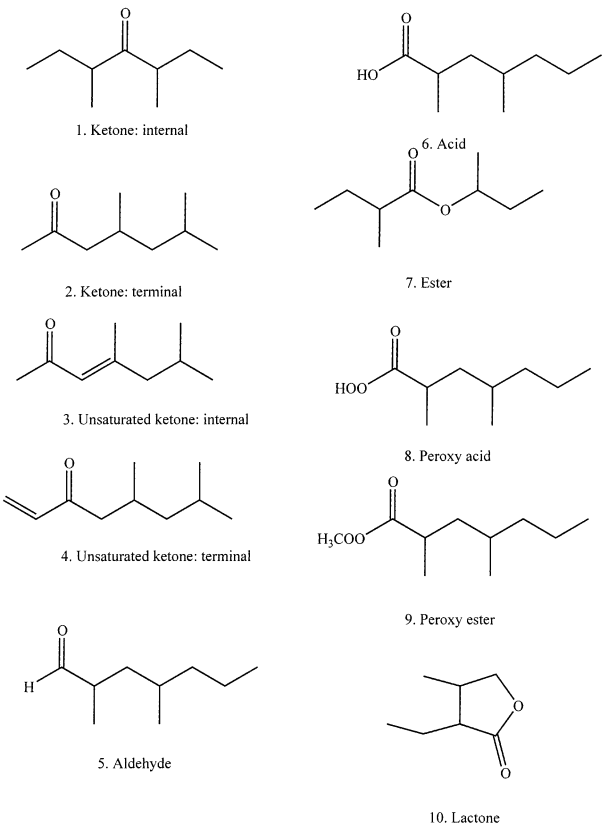

Figure 6. Structures of the PP-type model systems.

The application of the same scaling procedure to the band at 1702 cm^{-1} leads to 1767 cm^{-1}, which is very similar to the calculated value for terminal unsaturated ketones. The application of the same procedure to the band at 1737 cm^{-1} gives 1803

TABLE 6: Assignment of the Various Bands Arising from the Deconvolution of the Relevant Region of the Spectrum of Photooxidized PP

exptl freq (cm^{-1})	
1702	unsaturated ketones
1712	carboxylic acid: dimeric form
1722	ketones
1735	ester
1758	peroxy acid or peroxy ester
1778	carboxylic acid (free form) or lactone

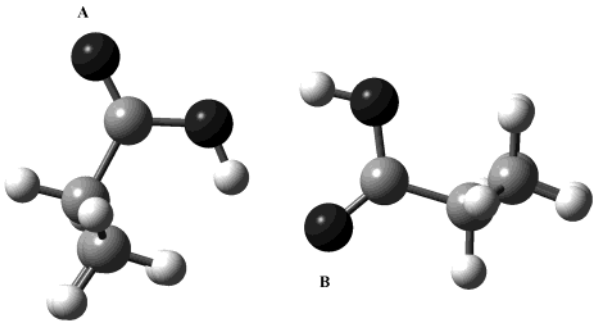

Figure 7. Structure of the model dimeric carboxylic acid system.

cm^{-1}, to 1758 cm^{-1} gives 1825 cm^{-1}, and to 1778 cm^{-1} gives 1846 cm^{-1}. From these data follows that the band at 1737 cm^{-1} can be attributed to esters or aldehydes, the band at 1758 cm^{-1} to peroxy acids (or esters), and finally the band at 1778 cm^{-1} to carboxylic acids (in their free form) or lactones (see Table 6 for a summary).

Let us comment on the band at 1712 cm^{-1}, which was attributed to the carbonyl stretching mode of carboxylic acids in their dimeric form (see ref 7). The presence of dimers of carboxylic acids follows from the evidence that high local concentrations of oxidized products can be present in oxidized polyolefins (see for example ref 18).

Geometry optimizations and frequency calculations on the dimeric system resulting from the model acid depicted in Figure 6 are quite expensive. To investigate this point, we will thus resort to the model dimeric acid system depicted in Figure 7 made of two monomeric units having a simplified lateral chain.

The calculations performed on the model dimer show, as expected, two normal modes associated with the carbonyl stretches: the one associated with the free carbonyl group (A in Figure 7) is at 1835 cm^{-1}, and the one associated with the hydrogen-bonded carbonyl group (B in Figure 7) is at 1760 cm^{-1}. By considering that the frequency of the (free) carbonyl stretching mode of the larger carboxylic acid PP-type considered in Figure 6 is 1847 cm^{-1}, we can assume that the "expected" frequency of the corresponding dimeric system may be obtained as follows (a similar procedure can also be applied to the extinction coefficient to determine the "expected" value for the large dimeric system reported in Table 5):

$$\nu_{CO}(\text{dimer}, h-\text{bond}, \text{large}) = \nu_{CO}(\text{dimer}, h-\text{bond}, \text{small})\frac{\nu_{CO}(\text{monomer}, \text{large})}{\nu_{CO}(\text{dimer}, \text{free}, \text{small})} \quad (2)$$

The resulting value is 1771 cm^{-1}, which if scaled by means of the ratio 1722/1789 gives 1705 cm^{-1}. By considering the approximations exploited here, this number is reasonably close to the frequency of the experimental band at 1712 cm^{-1}, which can thus be assigned to dimeric carboxylic acids.

The assignments resulting from our procedure (see Table 6 for a summary) are in good agreement with respect to results presented in refs 6 and 7 (compare Table 2), where the assignment was done by resorting to chemical derivatization.

To close the discussion on PP, it is worth noticing that in our case, due to the weak oxidation conditions used, it is probably more likely that peracids and carboxylic acids result from the oxidation, more than peresters or lactones, which imply a further degree of oxidation.

TABLE 7: Assignment of the Various Bands Arising from Deconvolution of the Relevant Regions of the Spectrum of Photooxidized PE

exptl freq (cm^{-1})	
1713	ketone: internal
1721	ketone: terminal
964	trans vinylene: $-CH{=}CH-$
909−993	vinyl $-CH{=}CH_2$
889	vinylidene $>C{=}CH_2$

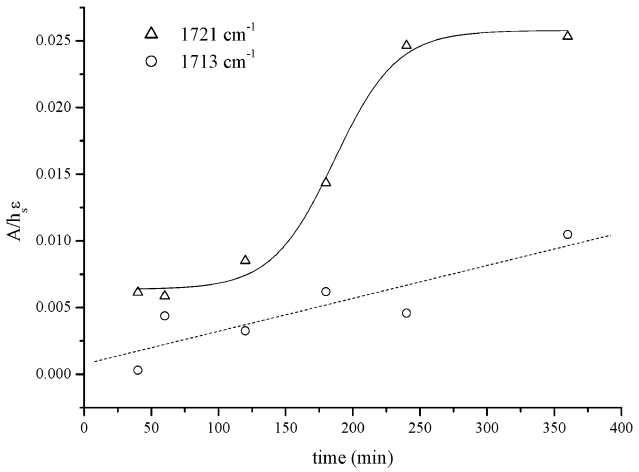

Figure 8. Evolution in time of the absorbance *A* of the bands resulting from the deconvolution corrected with the molar absorption coefficient ϵ of the species assigned to them. h_s is the height of the reference band. PE, C═O stretching band.

Moving to PE (Table 4), by following a procedure similar to that just presented, the band at 1713 cm^{-1} can be assigned to internal ketones and the one at 1721 cm^{-1} to terminal ketones. Switching to the region of the carbon double bond rocking and following ref 5, the bands at 964 and 889 cm^{-1}, whose intensity decreases as the irradiation time increases, can be assigned to *trans* vinylene groups ($-CH{=}CH-$) and to vinylidene groups ($>C{=}CH_2$), which are already present in the polyolefin. On the other hand, the bands at 909 and 993 cm^{-1} are due to vinyl groups ($-CH{=}CH_2$), which are formed as a result of the oxidation process. A summary of the assignment for PE is reported in Table 7.

We have just done the first step that we described in the methodological part, i.e., the assignment of the bands. The next step is to determine, at least in a semiquantitative way, the behavior of the concentrations of the various species formed in the photooxidation process and also to make an estimate of their quantity.

4.3. An Attempt to Quantify the Photooxidation Process. To quantify the oxidation process, we will resort to eq 1. To this end the molar absorption coefficients of the various species are required, which, in our case, have been taken from the calculations (see Tables 4 and 5).

Figures 8, 9, and 10 show the time evolution of the absorbance of the various bands corrected for the molar absorption coefficient of the appropriate species. The values on the *y*-axis are referred to as the height h_s of the absorption bands at 1304 cm^{-1} for PE and 1256 cm^{-1} for PP (see section 3).

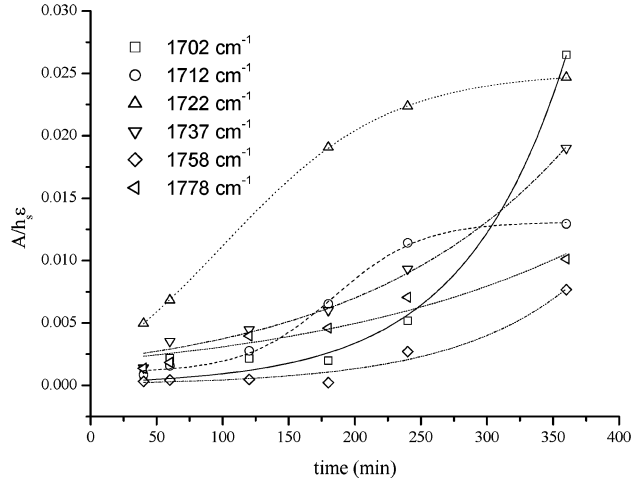

Figure 9. Evolution in time of the absorbance *A* of the bands resulting from the deconvolution corrected with the molar absorption coefficient ϵ of the species assigned to them. h_s is the height of the reference band. PP, C═O stretching band.

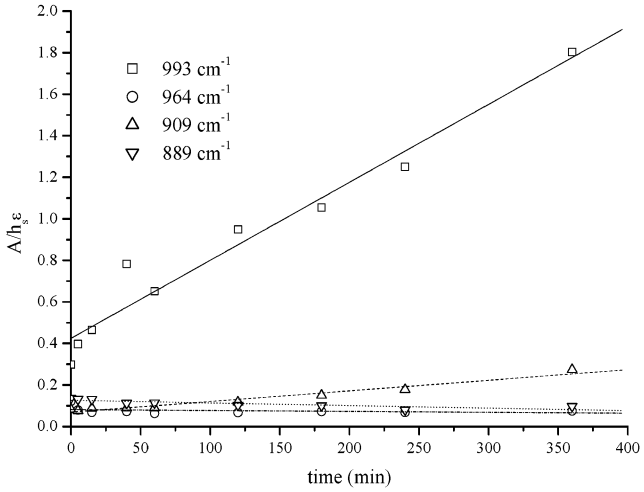

Figure 10. Evolution in time of the absorbance *A* of the bands resulting from the deconvolution corrected with the molar absorption coefficient ϵ of the species assigned to them. h_s is the height of the reference band. PE, C═C rocking.

Oxidized PE (Figure 8) shows an increase of both the bands at 1713 and 1721 cm^{-1}, which, as we have previously shown, refer to internal and terminal ketones, respectively (see Table 7). The observed trends in the relative absorbances are different, the band at 1713 cm^{-1} increasing almost linearly and the one at 1721 cm^{-1} having a sigmoidal trend. In the region of the carbon−carbon double bonds (Figure 10) the bands at 964 cm^{-1} (*trans*-vinylene) and 998 cm^{-1} (vinilydene) show a moderate decrease, which is consistent with a degradation of the vinylene and vinilydene groups already present in the PE samples.

A rapid increase of the bands at 909 and 993 cm^{-1}, connected to vinyl groups, is also evidenced, in accordance with previous findings (see for example refs 19 and 5), showing that in the case of photooxidation the dominant unsaturation coming from the oxidation process is vinyl. In particular, as shown by the same authors, the vinyl groups result from a Norrish type II photolysis of internal ketones (see Scheme 1).[20]

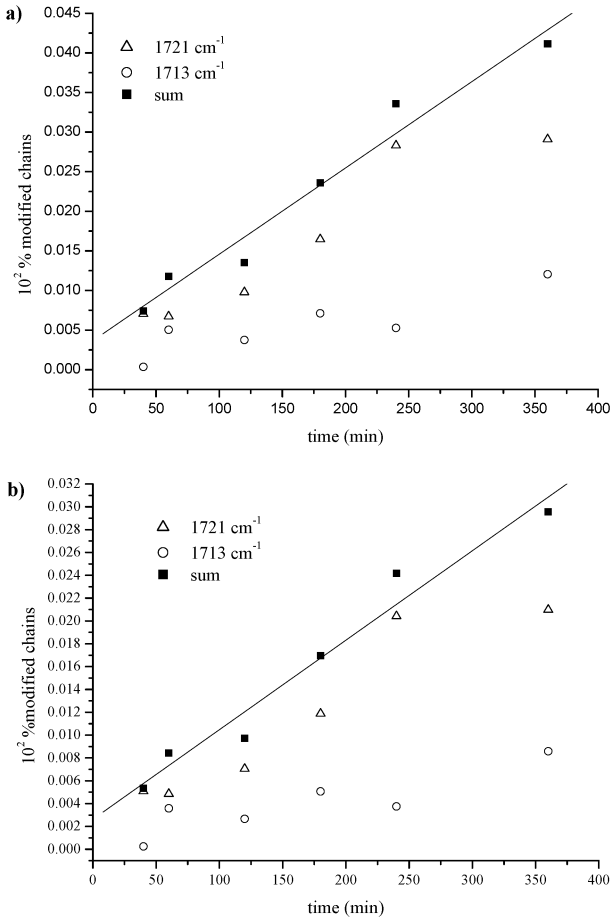

Figure 11. Evolution in time of the percentage of modified chains resulting from the various bands: (a) in vacuo; (b) with account of medium effects. PE, C═O stretching band.

The bands at 1713 and 1721 cm^{-1} (terminal and internal ketones) suggest that, at low exposure times, small quantities of internal and terminal ketones are produced directly by the oxidation process. At larger exposure times such quantities increase, but the increment of terminal ketones is much larger than that of internal ones. Such a behavior can be explained in terms of the Norrish type II photolysis: in fact, once internal ketones are formed, a part of them will undergo the photolysis process giving rise to terminal ketones and vinyl groups (the bands of the vinyl groups increase as well). From our results, it seems reasonable to infer that the Norrish type II photolysis occurs only when a given amount of internal ketones is formed. After that, the amount of internal ketones increases slowly, whereas the amount of terminal ketones rises and seems to reach a plateau.

Notice that our measurements do not evidence any increase in the vinylene band, which would be connected to the conver-

SCHEME 1: Norrish Type II Photolysis

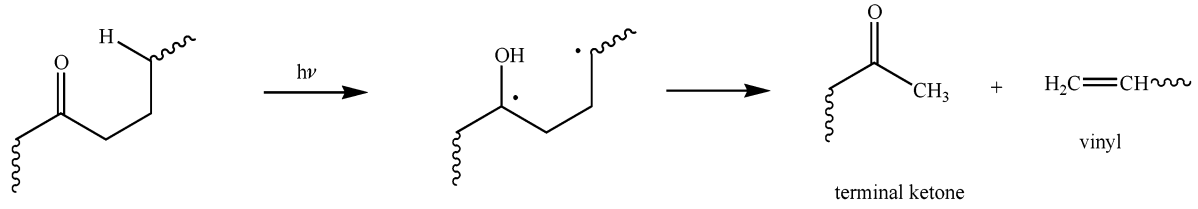

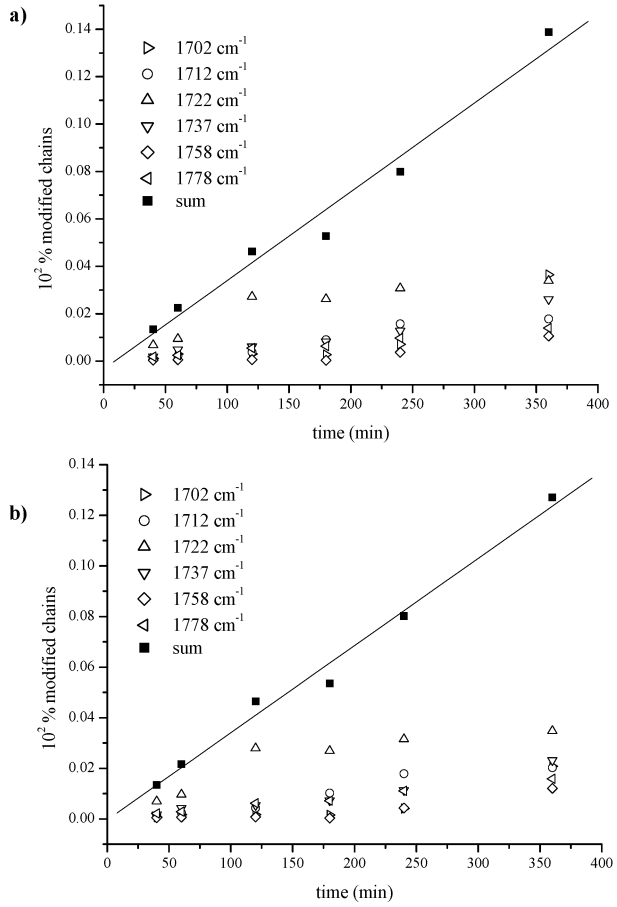

Figure 12. Evolution in time of the percentage of modified chains resulting from the various bands: (a) in vacuo; (b) with account of medium effects. PP, C═O stretching band.

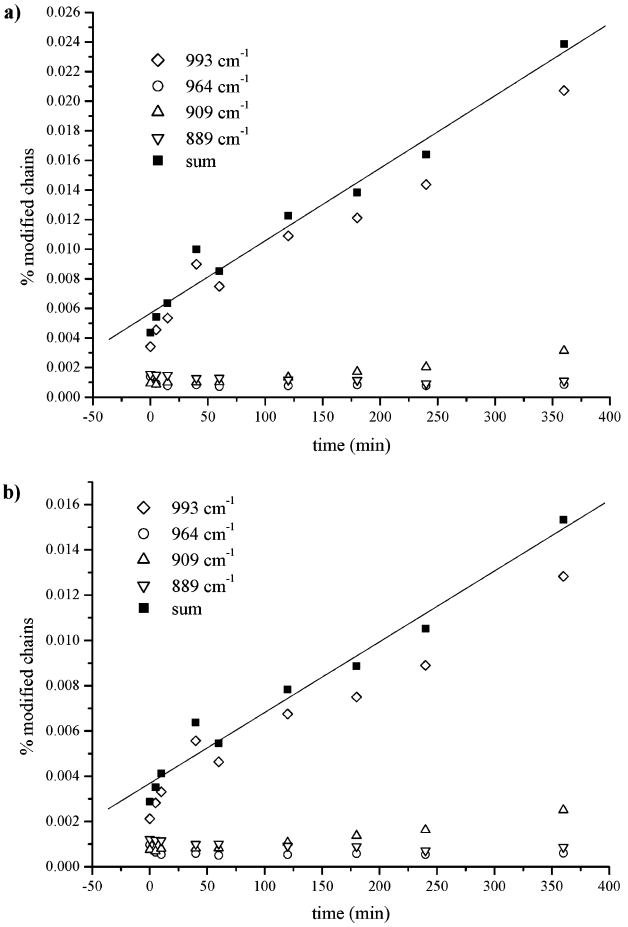

Figure 13. Evolution in time of the percentage of modified chains resulting from the various bands: (a) in vacuo; (b) with account of medium effects. PP, C═C rocking. The sum was done only over the bands at 993 and 909 cm^{-1}.

sion of vinyl groups into vinylene groups (see for example ref 19).

PP (Figure 9) shows an increase in the absorbances of all the bands. The largest increases are noticed for all the types of ketones (unsaturated, 1702 cm^{-1}; internal and terminal, 1722 cm^{-1}). In particular, while internal and terminal saturated ketones increase and seem to reach a plateau, unsaturated ketones increase exponentially. The increase of the band at 1735 cm^{-1} (attributed to esters) is also remarkable, whereas the bands at 1712, 1758, and 1778 cm^{-1}, assigned to higher oxidized products (peracids, peresters, carboxylic acids, or lactones), increase only slowly. This behavior seems reasonable, since we are focusing on mild photooxidation conditions.

Starting from the data mentioned so far, it is also possible to calculate the percentage of modified chains containing each functional group, as well as the total percentage of modified chains. In Figures 11a, 12a, and 13a we report the evolution in time of the percentage of modified chains as resulting from the analysis of each band and the total percentage of modified chains.

Focusing on the sum of modified chains (see Table 8), as obtained by considering the variation of the whole carbonyl band, we note that after 6 h of exposure under our conditions the ratio between C═O oxidized chains for PP and PE is more than 3, this showing a much greater oxidizability of PP with respect to PE. Much larger is the percentage of PE chains that oxidize to form C═C double bonds: in particular the ratio between C═C and C═O oxidized chains for PE is around 58. These findings are not surprising, being well documented in the literature (see for example ref 1).

TABLE 8: Percentages of Modified Chains for PP and PE, Given as the Sum of All Kinds of Oxidation Products

	A: isolated molecule	B: with medium effects
PE (carbonyl)	0.041×10^{-2}	0.030×10^{-2}
PP	0.139×10^{-2}	0.127×10^{-2}
PE (rocking)	2.386×10^{-2}	1.534×10^{-2}

4.4. A Further Refinement: Introducing Medium Effects. As a further refinement in our treatment and to complete the description of our methodology, we report in Figures 11b, 12b, and 13b the trend in the percentage of modified chains as obtained by considering medium effects in the theoretical calculations.

The estimated percentages of oxidized chains decrease if medium effects are considered (Table 8). This is not surprising because absorption coefficients calculated in the condensed phase are larger than the corresponding ones for isolated molecules. Looking at Tables 4 and 5 in more detail, we note that the ratios between the corresponding absorption coefficients calculated for the isolated systems and in the condensed phase are not constant. This influences the relative percentages, and in particular we note that the ratio between PP and PE C═O modified chains increases to around 4 and the ratio between C═C and C═O oxidized chains for PE decreases to around 52. Even if in this case the differences arising from the account of medium effects are not very large and do not change our findings (at least qualitatively), they can be larger in other cases: this should be considered if the methodology is applied in a strictly quantitative way.

5. Summary and Conclusions

We have proposed a methodology, which combines experimental evidence and theoretical calculations, to obtain a molecular interpretation and a quantitative analysis on photooxidation of polyolefins. The methodology has been tested against photooxidized polyethylene (PE) and polypropylene (PP) films but is generally applicable to any kind of polymers and oxidation conditions (gamma or UV irradiation, thermal oxidation).

While the chemical modifications on the examined polymers were obtained by irradiation, the results of the present work have a more general relevance. Indeed the detailed assignment of the vibrational bands to specific functional groups and the theoretical interpretation and evaluation are very useful to examine the "chemical status" of these important materials after being subject to different applicative conditions which can be in some way responsible for chemical aging.

The combination of experimental data and theoretical calculations may also be helpful in gaining information about other fields of polymer science: for example it is straightforward to apply the methodology we have described to other problems (i.e., the determination of functionalization rates) where the knowledge of extinction coefficients of nonisolable compounds is necessary. In addition, other spectroscopic quantities can be easily extracted from computations and the combination of theory and experiment can open a wide range of possible studies.

With regard to the quality of the results that can be obtained, we think that the present application is a good test, yielding results in good agreement with previous findings obtained by exploiting only experimental evidence.

Acknowledgment. The authors would like to thank Prof. Francesco Ciardelli for helpful discussions and revising the manuscript.

References and Notes

(1) (a) Ranby, B.; Rabek, I. E. *Photodegradation and Photostabilization of Polymers: Principles and Applications*; Wiley: New York, 1975. (b) Scott, G., Ed. *Mechanisms of Polymer Degradation and Stabilization*; Elsevier: London, 1990. (c) Billingham, N. C., Chien, J. C. W., Eds. *Polymer Degradation and Stability, Vol. 44*; Elsevier: New York, 1994.

(2) (a) Davidson, R. G. *Polymer Degradation Studies by FT-IR*; Progress in Pacific Polymeric Science 2, Proceedings of the Pacific Polymer Conference, 1992. (b) Koenig, J. L. *Spectroscopy of Polymers*; American Chemical Society, Washington, DC, 1991. (c) Koenig, J. L. *Infrared and Raman Spectroscopy of Polymers*; Rapra Technology: Shawbury, 2001.

(3) Philippart, J.-L.; Posada, F.; Gardette, J.-L. *Polym. Degrad. Stab.* **1995**, *49*, 285.

(4) Vaillant, D.; Lacoste, J.; Dauphin, G. *Polym. Degrad. Stab.* **1994**, *45*, 355.

(5) Lacoste, J.; Carlsson, D. J. *J. Polym. Sci. A* **1992**, *30*, 493.

(6) Lacoste, J.; Valillant, D.; Carlsson, D. J. *J. Polym. Sci. A* **1993**, *31*, 715.

(7) Philippart, J.-L.; Sinturel, C.; Arnaud, R.; Gardette, J.-L. *Polym. Degrad. Stab.* **1999**, *64*, 213.

(8) Scott, A. P.; Radom, L. *J. Phys. Chem.* **1996**, *100*, 16502.

(9) Halls, M. D.; Schlegel, H. B. *J. Chem. Phys.* **1998**, *109*, 10587.

(10) Goddard, W. A., III; Cagin, C.; Blanco, M.; Vaidehi, N.; Dasgupta, S.; Floriano, W.; Belmares, M.; Kua, J.; Zamanakos, G.; Kashihara, S.; Iotov, M.; Gao, G. *Comput. Theor. Polym. Sci.* **2001**, *11*, 329.

(11) Tomasi, J.; Persico, M. *Chem. Rev.* **1994**, *94*, 2027.

(12) Cappelli, C.; Corni, S.; Tomasi, J. *J. Phys. Chem.* **2001**, *105*, 10807.

(13) Tomasi, J.; Cammi, R.; Mennucci, B.; Cappelli, C.; Corni, S. *Phys. Chem. Chem. Phys.* **2002**, *4*, 5697.

(14) (a) Spadaro, G.; Calderaro, E.; Rizzo, G. *Acta Polym.* **1989**, *40*, 702. (b) Gugumus, F. *Polym. Degrad. Stab.* **1996**, *53*, 161. (c) Gugumus, F. *Polym. Degrad. Stab.* **1998**, *62*, 245.

(15) Cammi, R.; Cappelli, C.; Corni, S.; Tomasi, J. *J. Phys. Chem. A* **2000**, *104*, 9874.

(16) Cappelli, C.; Corni, S.; Cammi, R.; Mennucci, B.; Tomasi, J. *J. Chem. Phys.* **2000**, *113*, 11270.

(17) Frisch, M. J.; Trucks, G. W.; Schlegel, H. B.; Scuseria, G. E.; Robb, M. A.; Cheeseman, J. R.; Zakrzewski, V. G.; Montgomery, J. A.; Stratmann, R. E.; Burant, J. C.; Dapprich, S.; Millam, J. M.; Daniels, A. D.; Kudin, K. N.; Strain, M. C.; Farkas, O.; Tomasi, J.; Barone, V.; Mennucci, B.; Cossi, M.; Adamo, C.; Jaramillo, J.; Cammi, R.; Pomelli, C.; Ochterski, J.; Petersson, G. A.; Ayala, P. Y.; Morokuma, K.; Malick, D. K.; Rabuck, A. D.; Raghavachari, K.; Foresman, J. B.; Ortiz, J. V.; Cui, Q.; Baboul, A. G.; Clifford, S.; Cioslowski, J.; Stefanov, B. B.; Liu, G.; Liashenko, C. A.; Piskorz, P.; Komaromi, I.; Gomperts, R.; Martin, R. L.; Fox, D. J.; Keith, T.; Al-Laham, M. A.; Peng, C. Y.; Nanayakkara, A.; Challacombe, M.; Gill, P. M. W.; Johnson, B.; Chen, W.; Wong, C. M. W.; Andres, J. L.; Gonzalez, C.; Head-Gordon, M.; Replogle E. S.; Pople, J. A. *Gaussian 99, Development Version* (Revision B09+); Gaussian Inc.: Pittsburgh, PA, 2000.

(18) (a) Billingham, N. C. *Makromol. Chem. Macromol. Symp.* **1989**, *24*, 145. (b) Celina, M.; George, G. A. *Polym. Degrad. Stab.* **1995**, *50*, 89.

(19) Arnaud, R.; Moisan, J.-Y.; Lemaire, J. *Macromolecules* **1984**, *17*, 332.

(20) Wayne, C. P.; Wayne, R. P. *Photochemistry*; Oxford University Press: Oxford, 1996.